

A Spin Polarization Transfer Approach to Intermolecular Interactions between Hydrocarbon Aromatic Compounds and Free Radicals

Aileen Lozán, Pedro Nieto, Sócrates Acevedo, and Vladimiro Mujica*

Universidad Central de Venezuela, Facultad de Ciencias, Escuela de Química. Apartado 47102, Caracas 1020A, Venezuela

Received: October 30, 2001; In Final Form: August 9, 2002

Using an effective spin-dependent Heisenberg Hamiltonian, we have modeled the interaction between closed-shell aromatic molecules and the free radical methyl. Physically, the model is based on a proportionality relationship, suggested by McConnell (McConnell, H. *J. Chem. Phys.* **1963**, *41*, 1910), between the product of the spin densities on each molecular fragment and the interaction energy of the system. The spin polarization, initially on the radical, is partly transferred to the molecule as the two fragments approach each other determining an effective spin interaction. The parameters of the effective Heisenberg-type Hamiltonian are determined through ab initio calculations of the electronic structure of the complex at the UMP2 level. Our calculations confirm the validity of a cage model recently proposed by Mujica et al. (Mujica, V.; Nieto, P.; Puerta, L.; Acevedo, S. *Energy Fuels* **2000**, *14*, 632) for spin trapping in fragments of asphaltenes while providing a consistent semiempirical approach to the interaction and stabilization problems.

1. Introduction

Asphaltenes are naturally occurring components of crude oil. They form a very complex colloidal mixture and are responsible for important industrial problems. Noticeable pipeline obstruction and other inconveniences in the processing of heavy crude are associated to asphaltene precipitation.

The presence of relatively high concentrations of free radicals in asphaltenes, a remarkable fact given the extremely reactive nature of these chemical species, has been verified by EPR measurements. To explain this phenomenon, Mujica et al. proposed a trapping mechanism in which the radicals are stabilized through the formation of aggregates.² This simple model encompasses many of the relevant experimental properties associated with asphaltene aggregation but it is entirely based on semiempirical quantum chemical modeling and molecular mechanics.

The first objective of this work is to examine the validity of the trapping model within an ab initio framework. This is of particular relevance given the importance of correlation effects in weakly bounded complexes involving free radicals and neutral fragments. Following the literature on electronic calculations involving free radicals and closed shell systems, we have used unperturbed Møller–Plesset second-order perturbation theory (UMP2) to include electronic correlation and compute the interaction energy,^{3–6} an approach that gives reasonable results for van der Waals complexes.^{7,8}

Our second goal is to present a model where the interaction between fragments are represented via an effective spin Hamiltonian of the Heisenberg type where the coupling parameters are obtained directly in terms of physical observables: the interaction energy and the local spin density. The model is based on one proposed by McConnell¹ to describe the interaction between two aromatic radicals and that has also been used for the description of magnetic properties of organic radical dimers.^{9–11} The basic idea is to express the interaction energy as a function of the spin density on each fragment and a

parameter that gauges the strength of the coupling between spins. This parameter is then computed from ab initio calculations. In addition, a linear correlation between the closed shell fragment polarizability and the spin density in the complex can be established, thereby providing a practical application of the spin model to more complex systems.

2. Effective Spin Model

In 1963, McConnell¹ proposed an effective Hamiltonian to describe the interaction energy between two aromatic radicals, labeled A and B,

$$H^{AB} = -\sum_{ij} J_{ij}^{AB} \vec{S}_i^A \cdot \vec{S}_j^B \quad (1)$$

where \vec{S}_i^A is an effective electronic spin of atom i in the molecule A and \vec{S}_j^B is similarly defined. By introducing the physically reasonable relationship connecting the effective spin to the spin density projected on atom i , ρ_i^A : $\vec{S}_i^A = \vec{S}^A \rho_i^A$,¹² one can then write eq 1 as

$$H^{AB} = -\vec{S}^A \cdot \vec{S}^B \sum_{ij} J_{ij}^{AB} \rho_i^A \rho_j^B \quad (2)$$

where \vec{S}^A and \vec{S}^B are the total spin angular momentum operators for the molecules A and B, respectively.

We can adapt McConnell's idea, which describes a multi-center problem, to one where only two sites are considered, each corresponding to a whole molecular fragment. Taking the quantum mechanical average in eq 2,

$$\langle H^{AB} \rangle = -\langle \vec{S}^A \cdot \vec{S}^B \rangle \sum_{ij} J_{ij}^{AB} \rho_i^A \rho_j^B \quad (3)$$

The interaction energy ΔE^{SM} between the two fragments can be calculated ab initio using the method of the supermolecule, which simply consists of computing separately the energies of the fragments A and B and of the complex (supermolecule)

formed by bringing the fragments to their equilibrium configuration and subtracting these values, that is

$$\Delta E^{SM} = E_{SM} - E_{M_A} - E_{M_B} \quad (4)$$

We also assume that the expectation value of the effective Hamiltonian (2), $\langle H^{AB} \rangle$ is equal to the interaction energy

$$\langle H^{AB} \rangle = \Delta E^{SM} \quad (5)$$

This assumption corresponds physically to representing all the distance dependence of the Hamiltonian by the effective spin operator, because ΔE^{SM} can also be written as

$$\Delta E^{SM} = E_{SM}(r) - E_{SM}(r \rightarrow \infty) \quad (6)$$

where r is the interfragment distance. This approach is very similar to that used by Löwdin to define the exchange integral.¹³ Similar approaches, based on Heisenberg effective spin operators, have been used extensively in the literature on magnetism¹⁴ but its ultimate justification in describing the dispersion interaction would be the comparison to the ab initio calculations and experimental results.

Combining eqs 3–5, we obtain

$$\Delta E^{SM} = -\langle \vec{S}^A \cdot \vec{S}^B \rangle \sum_{ij} J_{ij}^{AB} \rho_i^A \rho_j^B \quad (7)$$

We further assume that all terms J_{ij}^{AB} are equal to J^{AB} , so that

$$\Delta E^{SM} = -\langle \vec{S}^A \cdot \vec{S}^B \rangle J^{AB} \sum_{i \in A} \rho_i^A \sum_{j \in B} \rho_j^B \quad (8)$$

where the sum over atomic indexes on each fragment, A or B , is the total spin density defined below by eq 12. We can introduce an effective coupling constant J_{AB}^{eff} through the eqs

$$\Delta E^{SM} = -\frac{1}{2} J_{AB}^{\text{eff}} \rho_A^s \rho_B^s \quad (9)$$

$$J_{AB}^{\text{eff}} = 2 \langle \vec{S}^A \cdot \vec{S}^B \rangle J^{AB} \quad (10)$$

The effective coupling is a function of the interfragment distance and orientation and is computed from the ab initio calculations in eq 9 as

$$J_{AB}^{\text{eff}} = \frac{-2\Delta E^{SM}}{\rho_A^s \rho_B^s} \quad (11)$$

This equation, together with the semiempirical expression (3), constitutes an extension of the original McConnell's formulation.

3. Computational Methodology

All ab initio calculations were carried out using GAUSSIAN 94¹⁵ and for the construction of the spin density maps MOLDEN¹⁶ was employed. The calculations were performed keeping the planar geometry of the fragments and displacing them along the coordinate perpendicular to the molecular planes as shown in Figure 1.

It is well-known that calculations of interaction energies at the Hartree–Fock level based on eq 4 must be corrected to account for the basis set superposition error (BSSE).¹⁷ Table 1 displays values of interaction energies for various separation distances between fragments of the methyl–benzene complex for different basis sets, with and without taking into account the BSSE. It is clear from this table that using the basis set

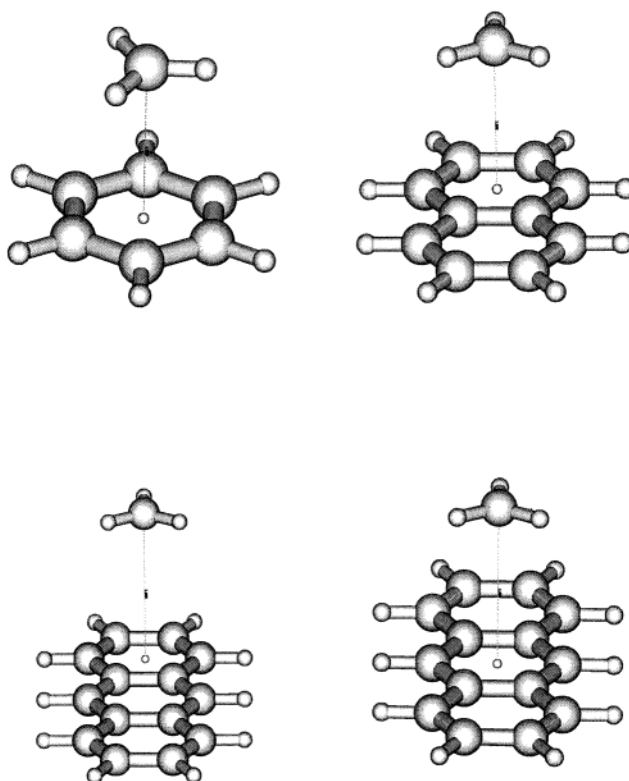


Figure 1. Radical complexes studied: (a) methyl–benzene, (b) methyl–naphthalene, (c) methyl–anthracene (geometry I), and (d) methyl–anthracene (geometry II).

TABLE 1: UMP2 BSSE Corrected and Uncorrected Values for Interaction Energies and Equilibrium Distances for Methyl Benzene Using UMP2 and Various Basis Sets

basis	R (Å)	ΔE (kcal/mol)	R_c (Å)	ΔE_c (kcal/mol)
6-31G	3.85	−0.26795	repulsive	repulsive
6-31G(d)	3.75	−0.40788	repulsive	repulsive
6-31G(d,p)	3.60	−0.54593	repulsive	repulsive
6-31+G(d)	3.75	−0.93499	4.20	−0.04392
6-31++G(d)	3.75	−1.15462	4.20	−0.06902
6-311G	3.90	−0.26983	repulsive	repulsive
6-311+G	3.75	−0.91616	repulsive	repulsive
6-311+G(d)	3.60	−1.11069	3.90	−0.11296

6-311+G(d) corrected for BSSE gives both comparable energies and similar interfragment potential energy surfaces to those obtained using a smaller basis set (6-31G) without taking into account the BSSE. This is in agreement with recent studies¹⁸ that show that for MP2-level calculations, like the one we are presenting here, the use of the conventional counterpoise correction of Boys and Bernardi is less justified than for the Hartree–Fock model. This is apparently due to cancellation of errors, but an unequivocal analysis of BSSE for all correlation levels is still lacking in the literature and a case-by-case numerical analysis seems to be required. Since we found a very consistent trend in using the two basis sets we feel justified in carrying out our calculations using a 6-31G basis without including the BSSE correction at the UMP2 level. Similar results have been found in more elaborated calculations with similar systems to the ones considered here.^{19–21}

Spin contamination was found to be consistent and small in all fragments at the relevant distances, thus making the use of the supermolecule method meaningful. For instance, typical values of the spin quantum number corresponding to S^2 are 0.7593 for CH_3^\bullet and between 0.7593 and 0.7597 for the radical fragments of Figure 1.

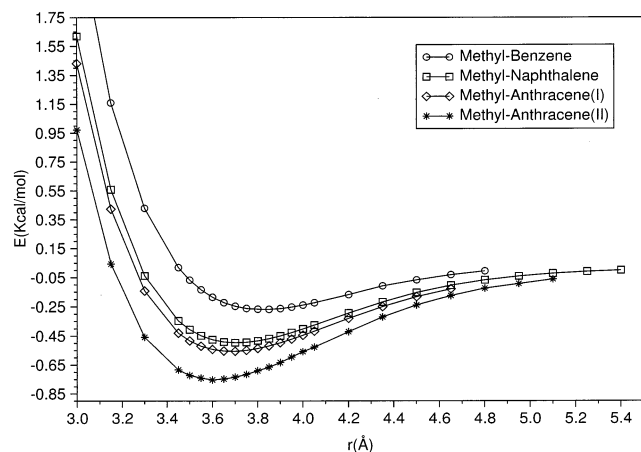


Figure 2. UMP2/6-31G interaction energy for each of the radical complexes in Figure 1 as a function of the interfragment distance.

TABLE 2: UMP2/6-31G Equilibrium Distances, Total Interaction Energies, and Interaction Energies per Carbon Atom for Methyl-Benzene, Methyl-Naphthalene, and Methyl-Anthracene Geometries I and II

complex	R (Å)	ΔE (kcal/mol)	$(\Delta E/N \text{ } ^\circ\text{C})$ (kcal/mol)
methyl-benzene	3.85	-0.26795	-0.03828
methyl-naphthalene	3.70	-0.49573	-0.04507
methyl-anthracene (I)	3.70	-0.55597	-0.03706
methyl-anthracene (II)	3.60	-0.75301	-0.05020

The net spin density on each fragment ρ_A^S for each complex (AB) considered in this work was calculated around the minima of the potential energy curve by adding the atomic spin densities $\rho_i^{A(B)}$ for all atoms in the fragment. Following Novoa et al.,²² who did not find significant differences by using more accurate integration procedures, we have calculated atomic densities according to a Mulliken analysis²³ of the UMP2/6-31G results:

$$\rho_A^S = \sum_{i \in A} \rho_i^A \quad (12)$$

4. Results and Discussion

4.1. Interaction Energies and Spin Densities. We have used methyl as the spin polarization transferring fragment. It was selected because it has a small enough number of electrons to be tractable with our computational means and, more important, because the spin density is localized on the carbon atom so that this fragment can be used as a sort of master probe for the study of polarization transfer. Figure 2 shows potential energy curves for the interaction between methyl and several hydrocarbons. They all exhibit a minimum at a distance, typical of van der Waals interactions, of roughly 3.8 Å. The resulting interaction energies and interfragment distances are summarized in Table 2, which also shows the interaction energy divided by the total number of carbon atoms for the supermolecule. The behavior of the stabilization energy per carbon atom indicates that larger complexes are more stable, a result that supports our conjecture that asphaltene aggregation is partially due to stabilization due to spin polarization transfer.

Figure 3 shows contour maps of the spin density at the equilibrium distance for each of the radical complexes shown in Figure 1. The spin polarization transfer from the methyl radical to the closed shell fragment is evident in these maps given the fact that the total spin density of the isolated closed shell hydrocarbons is zero. Rings act as sinks of spin density and those closer to the methyl fragment are more affected as

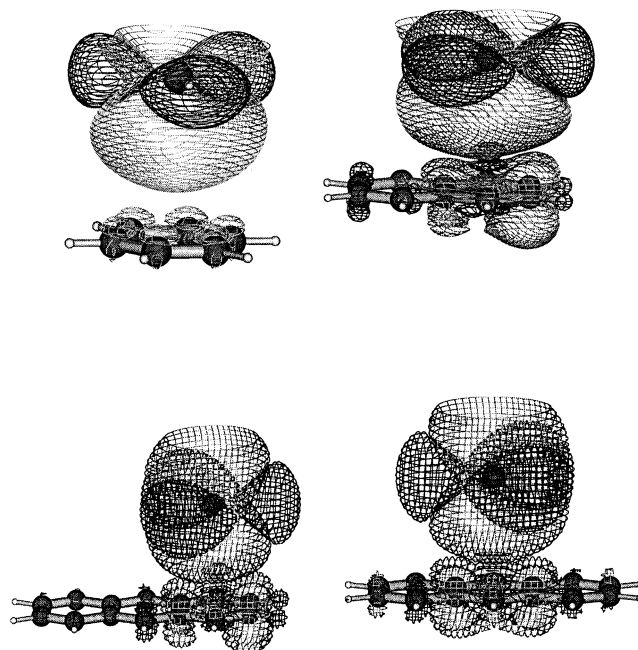


Figure 3. Contour maps of the UMP2/6-31G spin density at the equilibrium distance for each of the radical complexes in Figure 1.

TABLE 3: UMP2/6-31G Total Induced Spin Densities for Benzene, Naphthalene, and Anthracene

R (Å)	benzene	naphthalene	anthracene (I)	anthracene (II)
3.00	0.007012	0.007584	0.007755	0.008300
3.15	0.005774	0.006198	0.006210	0.006706
3.30	0.004700	0.005011	0.005090	0.005378
3.45	0.003736	0.003965	0.004017	0.004225
3.60	0.002880	0.003041	0.003078	0.003224
3.75	0.002140	0.002253	0.002275	0.002378
3.90	0.001527	0.001605	0.001619	0.001688
4.05	0.001048	0.001098	0.001107	0.001152
4.20	0.000690	0.000722	0.000729	0.000756
4.35	0.000437	0.000456	0.000459	0.000477

shown for the two different geometries of the methyl-anthracene complex.

Table 3 contains total spin densities induced on benzene, anthracene (geometries I and II), and naphthalene as a function of the interfragment distance. This results show that the induced polarization increases as a function of the number of benzene rings and that it is strongly dependent on the relative position of the fragments as shown by the difference for the two geometries of the anthracene-methyl complex. These effects are also represented in Figure 4 that contains plots of the induced spin density for various distances.

From the examination of the results for the two geometries involving the anthracene fragments, we conclude that the interaction energy increases as a function of transferred spin polarization. A result that could have been expected given the polarizable nature of the hydrocarbon fragments involved in our calculations.

We also calculated the interaction energy for two complexes, benzene/methyl and benzene/ethylene, for two geometrical configurations as shown in Figure 5. The distances between fragments were varied symmetrically with respect to the central fragment. Table 4 contains values of the interaction energy, stabilization energy per carbon atom at the equilibrium distance for the different complexes. The corresponding result for the benzene/benzene complex is given as a reference. Parts a and b of Figure 6 respectively display the interaction energy curves as a function of the interfragment distance for supermolecules

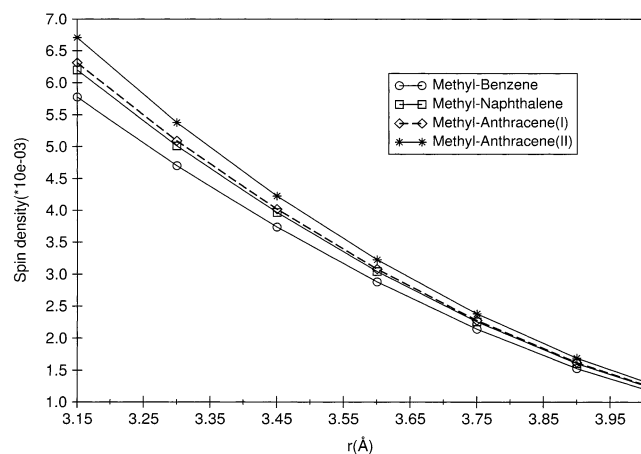


Figure 4. Induced UMP2/6-31G spin density for various distances for each of the radical complexes.

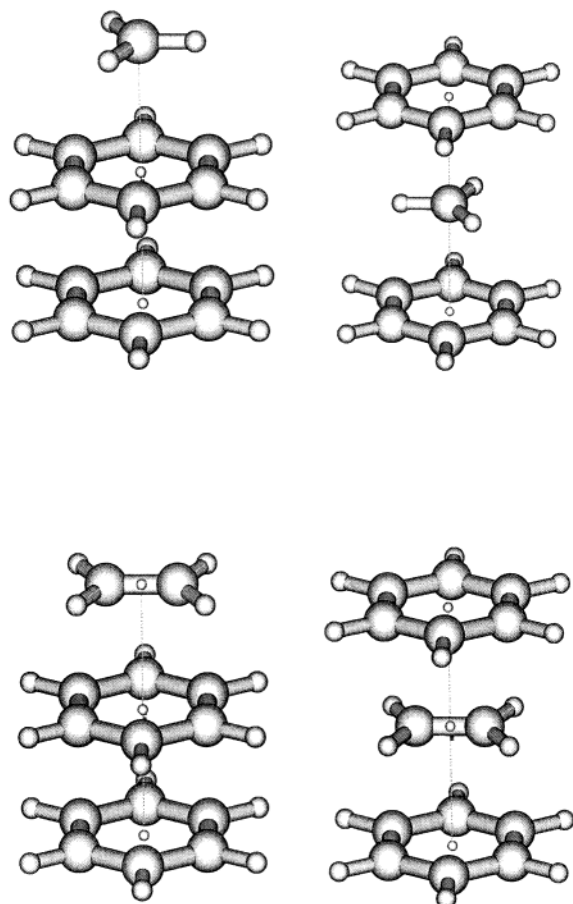


Figure 5. Geometries for the (a) benzene–benzene–methyl, (b) benzene–methyl–benzene, (c) benzene–benzene–ethene, and (d) benzene–ethene–benzene.

a and b, respectively c and d, in Figure 5. We found that the interaction energy per carbon atom is larger in both complexes where the radical methyl is involved than those with the closed shell fragment ethylene, a result consistent with the fact that stabilization increases with spin polarization transfer. For the benzene-benzene system, the interaction energy goes from a negative value at 3.80 Å to zero at 7.6 Å (see Table 5) indicating that both methyl and ethylene mediate a favorable interaction with methyl exerting the largest influence.

4.2. Atoms in Molecules: Analysis and the Nature of the Bonding Interaction. The analysis of the electronic density for

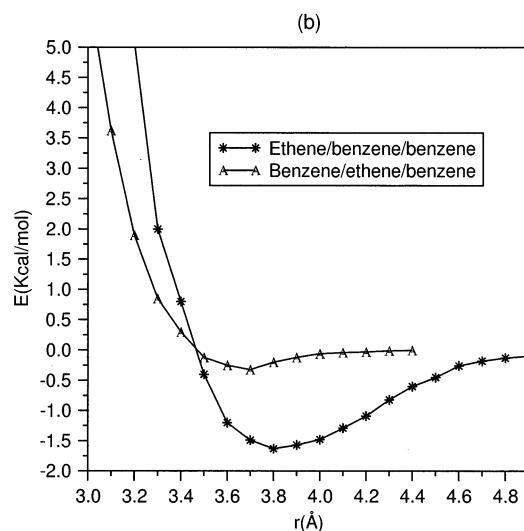
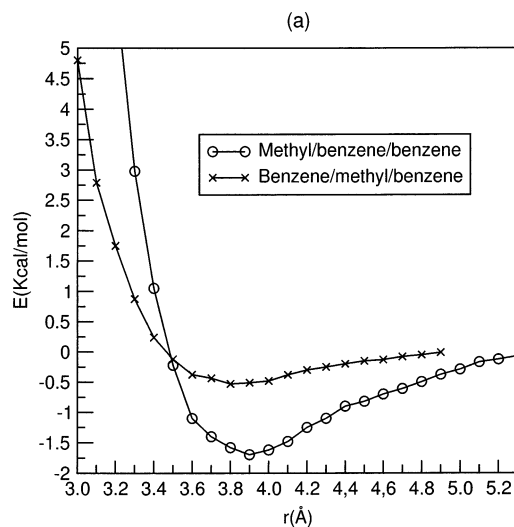


Figure 6. UMP2/6-31G interaction energy for the complexes formed out of the fragments, benzene, methyl, and ethene.

TABLE 4: Total Interaction Energy, Equilibrium Distance, and Interaction Energy per Carbon Atom for the Complexes Shown in Figure 5 and the Benzene–Benzene Complex in Its Stacked Configuration

complex	R (Å)	ΔE (kcal/mol)	$(\Delta E/N \text{ } ^\circ\text{C})$ (kcal/mol)
methyl–benzene–benzene	3.90	–1.69616	–0.13047
benzene–methyl–benzene	3.80	–0.53188	–0.04014
ethylene–benzene–benzene	3.80	–1.63153	–0.11654
benzene–ethene–benzene	3.70	–0.32292	–0.02307
benzene–benzene	3.90	–1.43951	–0.12001

TABLE 5: Interaction Energies for Two Relevant Distance for the Benzene–Benzene Complex

complex	R (Å)	ΔE (kcal/mol)	$(\Delta E/N \text{ } ^\circ\text{C})$ (kcal/mol)
benzene–benzene	3.80	–1.38303	–0.11525
benzene–benzene	7.60	≈ 0	≈ 0

the methyl–benzene and methyl–ethylene systems provides further insight into the nature of the interaction between these fragments.

Following Bader,²⁴ we have performed a topological analysis of the electronic density using the information provided by the gradient and laplacian fields. Specifically, we characterized the interaction by determining the value of the electronic density,

TABLE 6: Quadratic Fitting Coefficients A , B , and C for the Curves J_{AB}^{EF} (Equation 14) for Each of the Complexes

complex	A	B	C
methyl–benzene	−2.0694	15.871	−29.932
methyl–naphthalene	−1.9533	14.508	−26.307
methyl–anthracene (II)	−2.0446	14.821	−26.113
average	−2.022	15.067	−27.451

the sign of the laplacian, and the ratio of curvatures at selected critical points of the density. As a representative region of the density, we choose the interatomic region connecting a carbon atom, in either the benzene or the ethylene molecule, with the carbon atom in the methyl radical.

The most important parameter to characterize the nature of the interaction is the ratio $\eta = |\lambda_1|/\lambda_3$ of curvatures along the bond direction and perpendicular to it, respectively. For strong covalent bonds, η lies between 1.3 and 2.5, whereas for weak van der Waals interactions, between closed shell systems, typical values of this parameter are between 0.15 and 0.25.²⁵

For the methyl–ethylene system a value of $\eta = 0.7$ is found, and the corresponding value is 0.8 for methyl–benzene. For the closed shell–closed shell system, ethylene–ethylene, a value of $\eta = 0.30$ is obtained. These results confirm our expectation that the open shell–closed shell interaction corresponds to a chemical bond whose strength is between that of a covalent and a vdW interaction. A similar result was found by Chalasinski et al.,⁸ using a different methodology. They characterized the bond between the closed shell–open shell systems He and CH[•] as an “incipient bond”, i.e., a bond of intermediate strength.

4.3. Model Hamiltonian and Parametrization. The introduction of an effective spin Hamiltonian leads to eq 9 that establishes a linear relationship between the interaction energy and the product of spin densities on each fragment, a result that is confirmed by our calculations.

We introduce a further approximation for the description of the effective interaction between fragments: the spin density is calculated at the equilibrium distance so that all the distance dependence is transferred to a function $J_{AB}^{EF}(r)$ of the interfragment distance r , that is

$$\Delta E^{SM} = -\frac{1}{2} J_{AB}^{eff} \rho_A^s \rho_B^s \approx -\frac{1}{2} J_{AB}^{EF}(r) \rho_A^{s,EQ} \rho_B^{s,EQ} \quad (13)$$

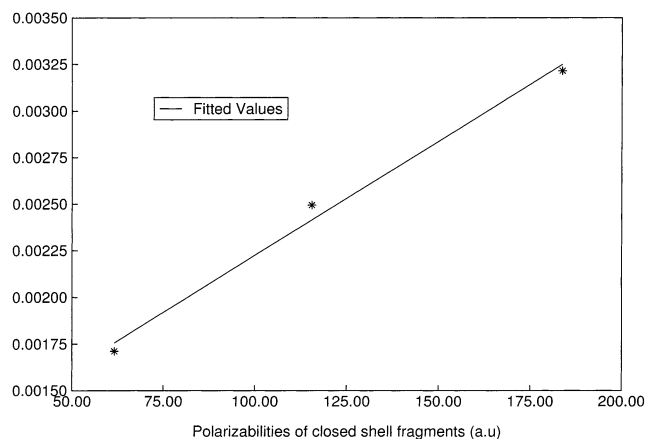
where $\rho_A^{s,EQ}$ and $\rho_B^{s,EQ}$ are the fragments' spin densities at the equilibrium distance.

With this approximation $J_{AB}^{EF}(r)$ can be fitted to a quadratic equation

$$J_{AB}^{EF} \approx Ar^2 + Br + C \quad (14)$$

The coefficients A , B , and C are weakly dependent on the fragments' chemical identities, and for qualitative purposes one can use the same values for the whole family of fragments. The results of the quadratic fit are summarized in Table 6.

Further insight into the nature of the spin dependent effective Hamiltonian can be gained by realizing that the product of the fragment spin densities at the equilibrium distance is linearly related to the polarizability of the closed shell fragment, a quantity readily available in the literature²⁶ for many organic molecules. Figure 7 shows this linear dependence and the values of the fitting parameters. This result can be understood by noticing that the dispersion interaction depends on the product of polarizabilities of the fragments involved.²⁷ Since the distance dependence of the energy is preserved in the description using the effective spin Hamiltonian, the existence of a linear

**Figure 7.** Product of the fragment spin densities at the equilibrium distance vs polarizability of the closed-shell fragments.**TABLE 7: A Comparison of *ab Initio* and Parametrized Interaction Energies**

complex	ΔE (kcal/mol)	ΔE_{param} (kcal/mol)
methyl–benzene	−0.26795	−0.34576
methyl–naphthalene	−0.49573	−0.48883
methyl–anthracene (II)	−0.75301	−0.64759
methyl–phenanthrene	−0.76674	−0.60163

relationship between the product of spin densities and the polarizability of the closed shell fragment (the radical fragment is kept constant) seems very plausible. A more quantitative argument will be presented elsewhere.²⁸

To show the internal consistency of our approach, we calculated the interaction energies between selected fragments using the expressions for J_{AB}^{EFF} and $\rho_A^{s,EQ} \rho_B^{s,EQ}$ in eqs 13 and 14. An equilibrium distance near 3.80 Å was obtained in all cases and the interaction energies are close to their *ab initio* values. The result of this comparison is shown in Table 7 which shows a reasonable agreement in all the cases considered here.

5. Conclusions

Our *ab initio* study supports the idea of a trapping stabilization mechanism² for radical species, i.e., the stabilization energy increases with system size. The magnitude of this energy is directly related to the degree of spin polarization induced on the closed shell molecular partner in the complex, a result that is in agreement with McConnell's criterion.

The introduction of an effective spin Hamiltonian can be used as an interpretative and computational tool for the kind of systems we are considering. This model description seems robust and could lend itself for the description of intermolecular interactions in more complex systems where van der Waals and dispersion forces may be dominant.

Acknowledgment. This research has been supported by CONICIT through Grants G97000722 and 97004022 and CDCH through Grants 03.124338/99 and 03.12.4087/98.

References and Notes

- (1) McConnell, H. *J. Chem. Phys.* **1963**, *41*, 1910.
- (2) Mujica, V.; Nieto, P.; Puerta, L.; Acevedo, S. *Energy Fuels* **2000**, *14*, 632.
- (3) Karlström, G. *Theor. Chim. Acta* **1983**, *105*, 3777.
- (4) Cunha, C.; Canuto, S. *Theochem.* **1999**, *494*, 73.
- (5) Pawliszyn, J.; Szczesniak, M.; Scheiner, S. *J. Phys. Chem.* **1984**, *88*, 1726.
- (6) Salhi-Benachenhou, N.; Engels, B.; Huang, M.; Lunell, S. *Chem. Phys.* **1998**, *236*, 53.

- (7) Cybulski, S. M.; Chalasinski, G.; Szczesniak, M. *J. Chem. Phys.* **1996**, *105*, 9525.
- (8) Chalasinski, G.; Klos, J.; Cybulski, S. *Collect. Czech. Chem. Commun.* **1998**, *63*, 1473.
- (9) Yamaguchi, K.; Fueno, T.; Nakasuji, N.; Murata, I. *Chem. Lett.* **1986**, *4*, 629.
- (10) Yamaguchi, K.; Namimoto, H.; Fueno, T. *Mol. Cryst. Liq. Cryst.* **1989**, *176*, 151.
- (11) Teki, Y.; Taku, T.; Itoh, K. *Mol. Cryst. Liq. Cryst.* **1995**, *271*, 213.
- (12) Pope, M.; Swenberg, C. *Processes in Organic Crystals and Polymers*; Oxford University Press: New York, 1999; p 1033.
- (13) Löwdin, P. O. *Rev. Mod. Phys.* **1962**, *34*, 80.
- (14) Madelung, O. *Introduction to Solid-State Theory*; Springer-Verlag: Berlin 1981.
- (15) Frisch, M. J.; Trucks, G. W.; Schlegel, H. B.; Scuseria, G. E.; Robb, M. A.; Cheeseman, J. R.; Zakrzewski, V. G.; Montgomery Jr., J. A.; Stratmann, R. E.; Burant, J. C.; Dapprich, S.; Millam, J. M.; Daniels, A. D.; Kudin, K. N.; Strain, M. C.; Farkas, O.; Tomasi, J.; Barone, V.; Cossi, M.; Cammi, R.; Mennucci, B.; Pomelli, C.; Adamo, C.; Clifford, S.; Ochterski, J.; Petersson, G. A.; Ayala, P. Y.; Cui, Q.; Morokuma, K.; Malick, D. K.; Rabuck, A. D.; Raghavachari, K.; Foresman, J. B.; Cioslowski, J.; Ortiz, J. V.; Stefanov, B. B.; Liu, G.; Liashenko, A.; Piskorz, P.; Komaromi, I.; Gomperts, R.; Martin, R. L.; Fox, D. J.; Keith, T.; Al-Laham, M. A.; Peng, C. Y.; Nanayakkara, A.; Gonzalez, C.; Challacombe, M.; Gill, P. M. W.; Johnson, B.; Chen, W.; Wong, M. W.; Andres, J. L.; Head-Gordon, M.; Replogle, E. S.; Pople, J. A. *Gaussian 94*, revision C.3; Gaussian, Inc.: Pittsburgh, PA, 1994.
- (16) Schaftenaar, G. *MOLDEN*, version 3.7; University of Nijmegen, Toernooiveld: The Netherlands, 1999.
- (17) Boys, S. F.; Bernardi, F. *Mol. Phys.* **1970**, *4*, 553.
- (18) Salvador, P.; Paizs, B.; Duran, M.; Suhai, S. *J. Comput. Chem.* **2001**, *22*, 765.
- (19) González, C.; Lim, E. C. *J. Phys. Chem. A* **2000**, *104*, 2953.
- (20) González, C.; Lim, E. C. *J. Phys. Chem. A* **2001**, *105*, 1904.
- (21) González, C.; Lim, E. C. *J. Phys. Chem. A* **2001**, *105*, 10583.
- (22) Novoa, J. J.; Mota, F.; Veciana, J.; Cirujeda, J. *Mol. Cryst. Liq. Cryst.* **1995**, *71*, 79.
- (23) Szabo A.; Ostlund, N. *Modern Quantum Chemistry. Introduction to Advanced Electronic Structure Theory*; MacMillan Publishing Co., Inc.: New York, 1982; p 151.
- (24) Bone, R. G. A.; Bader, R. F. W. *J. Phys. Chem.* **1996**, *26*, 10892.
- (25) Bader, R. *Atoms in Molecules. A Quantum Theory*; Clarendon Press: Oxford, 1990.
- (26) Ahmed, G. *Adv. Chem. Phys.* **1993**, *123*, 415.
- (27) Landau, L. D.; Lifshitz, E. M. *Quantum Mechanics: Nonrelativistic Theory*; Pergamon Press: Oxford, 1977.
- (28) Mujica, V.; et al. To be submitted.